The Immunostimulatory Activity of Unmethylated and Methylated CpG Oligodeoxynucleotide Is Dependent on Their Ability To Colocalize with TLR9 in Late Endosomes

Susan D. de Jong, Genc Basha, Kaley D. Wilson, Mikameh Kazem, Pieter Cullis, Wilf Jefferies and Ying Tam

J Immunol 2010; 184:6092-6102; Prepublished online 28 April 2010;
doi: 10.4049/jimmunol.0802442
http://www.jimmunol.org/content/184/11/6092

The Journal of Immunology is published twice each month by
The American Association of Immunologists, Inc.,
9650 Rockville Pike, Bethesda, MD 20814-3994.

Print ISSN: 0022-1767 Online ISSN: 1550-6606.

The Immunostimulatory Activity of Unmethylated and Methylated CpG Oligodeoxynucleotide Is Dependent on Their Ability To Colocalize with TLR9 in Late Endosomes

Susan D. de Jong,* Genc Basha,*,†,1 Kaley D. Wilson,*,1 Mikameh Kazem,* Pieter Cullis,* Wilf Jefferies,†,2 and Ying Tam‡,2

TLR9 recognizes CpG motifs present in pathogenic DNA and triggers potent immune responses. It is generally accepted that TLR9 distinguishes pathogenic DNA based, in part, on methylation status, where TLR9 binds unmethylated but not methylated CpG. However, we showed that methylated CpG induces potent TLR9-mediated responses when delivered in lipid nanoparticles. In this article, we report that methylation dictates the ability of free CpG DNA to colocalize with TLR9 in late endosomes. However, when delivered in lipid nanoparticles, CpG DNA and TLR9 colocalize, regardless of methylation status. Therefore, it is proposed that the ability of immune cells to distinguish unmethylated pathogenic from methylated mammalian DNA is controlled by a mechanism that regulates TLR9 mobilization and colocalization rather than a differential binding affinity. ***The Journal of Immunology*****, 2010, 184: 6092–6102.**

The mammalian immune system has evolved highly conserved pattern recognition receptors (PRRs), such as the TLR family, which recognize specific molecular patterns, expressed by a diverse group of infectious microorganisms, as danger signals of infection and trigger potent, protective immune responses (1–6). Inherent to this detection system is the ability to distinguish pathogen-associated patterns from those encountered during benign or beneficial self and environmental interactions. Although this can be easily conceptualized for TLRs 4, 2/6, and 5, all of which recognize structurally complex and unique ligands, such as LPS, peptidylglycan, and flagellin, it is somewhat less intuitive for TLR9, which specifically recognizes CpG DNA motifs (7).

Distinguishing pathogenic from eukaryotic DNA is a multifactorial process, relying on localization of TLR9 to the endosomal compartment (8, 9), suppression of CpG frequency in eukaryotic DNA, the occurrence of eukaryotic CpGs within immunosuppressive flanking sequences, and methylation status (2, 10, 11). With regard to methylation status, TLR9 was shown to specifically respond to unmethylated CpG motifs, such as those present in bacterial DNA, compared with eukaryotic CpGs, of which 70–80% are methylated (12). Furthermore, it was demonstrated that methylation of immunostimulatory CpG DNA abrogates activity, which is commonly attributed to the specificity of TLR9 for unmethylated motifs and its relative inability to bind methylated sequences. Direct evidence for this comes from surface plasmon resonance studies that reported higher-affinity binding of TLR9 with unmethylated CpG oligodeoxynucleotide (ODN) and CpG-containing plasmid DNA compared with the methylated forms (10, 13).

Conversely, it was demonstrated that when expressed on the cell surface, a chimeric TLR9 is capable of responding to self-DNA (9), and our group and other investigators observed that methylated CpG (mCpG) ODN possesses TLR9-mediated immunostimulatory potential when delivered in a lipid carrier system (14–16). Specifically, we recently reported that for natural phosphodiester and modified phosphorothioate ODN, lipid nanoparticle (LN) delivery endows mCpG ODN with immunostimulatory activity similar to or greater than the equivalent unmethylated ODN through a TLR9-mediated mechanism (17).

The ability of mCpG DNA to induce TLR9-mediated immune responses suggests that methylation status may determine the immunostimulatory activity of CpG DNA by mechanisms other than by affecting binding properties. We show in this article that although methylated and unmethylated CpG ODN in free form are taken up and traffic to the endosome similarly, only unmethylated ODN promotes effective mobilization of TLR9 to the late endosomal compartment, allowing for colocalization with its CpG ligand. Interestingly, administration of methylated and unmethylated CpG ODN in LNs, as well as empty LNs, promotes the mobilization of TLR9 to the endosome. We further demonstrate that following exposure to free unmethylated CpG ODN and LNs, colocalization occurs through an src-family kinase (SFK)-mediated signaling pathway. These results suggest that the lack of immunological activity for free methylated ODN is largely due to a failure to localize with TLR9 in the late endosomal compartment, rather than an inability to bind and activate TLR9. Finally, we confirm this hypothesis by showing that predosing with empty LNs to induce TLR9 mobilization to the endosomal

*Department of Biochemistry and Molecular Biology and †Biomedical Research Centre, University of British Columbia, Vancouver; and ‡Tekmira Pharmaceuticals, Burnaby, British Columbia, Canada

[1]G.B. and K.D.W. contributed equally to this work.

[2]W.J. and Y.T. are cosenior authors.

Received for publication July 24, 2008. Accepted for publication March 19, 2010.

This work was supported in part by Canadian Institutes for Health Research operating grants to P.R.C. and W.J. S.D.deJ. and K.D.W. were recipients of Natural Sciences and Engineering Research Council and Natural Sciences and Engineering Research Council, Canadian Institutes for Health Research, and Michael Smith Foundation for Health Research postgraduate awards, respectively.

Address correspondence and reprint requests to Dr. Ying K. Tam at the current address: AlCana Technologies, Inc., 2714 West 34th Avenue, Vancouver, British Columbia, V6L 2A1 Canada. E-mail address: ytam@alcanatech.com

The online version of this article contains supplemental material.

Abbreviations used in this paper: 1,19dioctadecyl3, 3,39,39 tetramethylindocarbocyanine perchlorate; BMDC, bone marrow dendritic cell; DC, dendritic cell; DiIC18, E, early; EEA1, early endosome Ag 1; ER, endoplasmic reticulum; LAMP1, lysosomal-associated membrane protein 1; L, late; LN, lipid nanoparticle; mCpG, methylated CpG; MFI, mean fluorescence intensity; ODN, oligodeoxynucleotide; PP2, pyrazol pyrimidine type 2; PRR, pattern recognition receptor; SFK, src-family kinase.

www.jimmunol.org/cgi/doi/10.4049/jimmunol.0802442

compartment endows free mCpG ODN with immunostimulatory activity.

The ability to differentiate between pathogenic and eukaryotic DNA represents a vital element of the eukaryotic immune system, promoting rapid and vigorous immune responses to protect against pathogenic attack while avoiding inappropriate and pathologic immune responses to self-DNA during normal processes, such as development, growth, and maintenance. Based on these data, we propose a new model in which the differential immunostimulatory activity of unmethylated and methylated CpG ODN, and, by extension, pathogenic and self-DNA, is determined by their ability to effectively induce mobilization of TLR9 and to colocalize with the receptor in the endosomal compartment, rather than differential affinities for TLR9. We suggest that discrimination between free methylated and unmethylated CpG ODN occurs upstream of TLR9 by recognition of the methylation status of free CpG ODN, triggering an SFK-signaling pathway that induces TLR9 mobilization to the late endosomal compartment. Uptake of LN systems also triggers TLR9 mobilization to the endosome, effectively bypassing this discrimination process and allowing for colocalization of the nucleic acid payload with TLR9, irrespective of methylation status.

Materials and Methods

Reagents

These studies were performed with phosphorothioated unmethylated and methylated (CpG motif shown in bold, 5′ methylcytosine denoted by *) INX-6295 (5′-TAA**C***G**TTGAGGGGCAT-3′), INX-5001 (5′-AA**C***G**TT-3′), CpG-2006 (5′-T**C***G**TC***G**TTTTGTC***G**TTTTGTC***G**TT-3′), and G3139 (5′-TCTCCCAG**C***G**TGC***G**CCAT-3′). Specific references to CpG and mCpG ODN in this section and *Results* refer to INX-6295, unless otherwise noted. Of note is the 3′ G-tetrad motif in INX-6295. Although immunostimulatory activity has been ascribed to these motifs, deletion or alteration did not have any impact on the immunostimulatory activity of INX-6295, whereas alteration of the CpG motif effectively abrogated activity. Unlabeled and 5′ FAM-labeled ODN were synthesized by Trilink BioTechnologies (San Diego, CA). Tissue culture media, L-glutamine, FBS, penicillin G, and streptomycin sulfate were from Invitrogen (Burlington, Ontario, Canada), and recombinant mouse IL-4 and GM-CSF were from Cedarlane Laboratories (Burlington, Ontario, Canada). BioPlex multiplex cytokine bead analysis reagents were purchased from Bio-Rad (Hercules, CA), and Abs for ELISA, cytometric bead array sets, and all Abs for flow cytometry were purchased from BD Biosciences (Mississauga, Ontario, Canada). Poly-D-lysine was from Sigma-Aldrich (Oakville, Ontario, Canada), Ficoll-Paque was from Amersham (Baie d'Urfe, Quebec, Canada), and collagenase D was obtained from Roche Applied Sciences (Laval, Quebec, Canada) The SFK inhibitor, pyrazol pyrimidine type 2 (PP2), was obtained from Calbiochem (San Diego, CA), and anti-CD11c MACS beads were from Miltenyi Biotec (Auburn, CA). Goat anti-mouse early endosome Ag 1 (EEA1) and rat anti-mouse lysosomal-associated membrane protein 1 (LAMP1) were from Santa Cruz Biotechnology (Santa Cruz, CA); rabbit anti-mouse to TLR3, TLR7, and TLR9 were obtained from Abcam (Cambridge, MA). Texas Red-conjugated dextran, 1,1′dioctadecyl3,3,3′,3′ tetramethylindocarbocyanine perchlorate ($DiIC_{18}$), and all secondary Abs were purchased from Invitrogen.

Mice and cell lines

Eight- to 10-wk-old female ICR and C57BL/6 mice were obtained from Charles River Laboratories (Wilmington, MA) and held in a pathogen-free environment. All procedures were approved by the appropriate institutional animal care committee (University of British Columbia and/or Tekmira Pharmaceuticals) and performed in accordance with the guidelines established by the Canadian Council on Animal Care. The murine macrophage cell line, RAW264.7, was obtained from the American Type Culture Collection (Manassas, VA) and cultured in DMEM supplemented with penicillin G (100 U/ml), streptomycin sulfate (100 μg/ml), 2 mM L-glutamine, and 10% FBS. Bone marrow dendritic cells (BMDCs) were derived from bone marrow cells collected from the long bones of ICR mice cultured with IL-4 and GM-CSF for 7 d in compete medium consisting of RPM1 1640 supplemented with penicillin G (100 U/ml), streptomycin sulfate (100 μg/ml), 2 mM L-glutamine, and 10% FBS. Resultant cells were >85% $CD11c^+$ and displayed a myeloid phenotype ($CD11c^+$, $CD11b^+$, $Mac3^{lo}$), as assessed by flow cytometry.

Preparation of liposomal nanoparticles

ODNs were encapsulated in LNs containing an ionizable aminolipid using an ethanol dialysis procedure, as previously described (18). $DiIC_{18}$ (0.5 mol%) was used in the formulation of empty LNs. Prior to formulation, CpG ODN was heated to eliminate any multimers (as assessed by PAGE) that may have formed, particularly for INX-6295 as a consequence of the 3′ G-tetrad. ODN concentrations were determined by UV spectroscopy (260 nm) on a Beckman DU 640 spectrophotometer, and lipid concentrations were determined using an inorganic phosphorus assay after separation of the lipids from the ODN by a Bligh and Dyer extraction (19). The ODN/lipid ratio was typically 0.10–0.13 (w/w), with a particle size of 100 ± 25 nm, as determined by quasi-elastic light scattering using a NICOMP Model 370 submicron particle sizer (Particle Sizing Systems, Santa Barbara, CA).

Cell uptake and immune response

For in vitro analysis, RAW264.7 or BMDCs were incubated for 1, 4, 12, or 24 h with 2–50 μg/ml fluorescently labeled free or encapsulated CpG ODN or mCpG ODN. Cells were harvested, washed, and then analyzed for uptake using flow cytometry. For ex vivo assessment, ICR mice were injected s.c. with 5 mg/kg fluorescently labeled free or encapsulated CpG ODN or mCpG ODN. Spleens and/or lymph nodes were obtained from mice 1, 4, 7, and 24 h postadministration. To demonstrate the role of SFK signaling in the immunostimulatory activity of CpG ODN, LN-CpG ODN, and LN-mCpG ODN, C57BL/6 mice were treated i.p. with 1 mg/kg PP2 twice per day for 7 d. PP2 has been extensively described and used in the literature as an SFK-specific inhibitor. Mice were injected i.v. with 20 mg/kg free or encapsulated fluorescently labeled CpG ODN or mCpG ODN, and tissue samples were collected 12 h postadministration. Cells were processed to single-cell suspensions, as previously described (20). For plasma cytokine analysis, blood was collected and processed to plasma by centrifugation and frozen at −20°C until assayed. Plasma concentrations of IL-6, MCP-1, and IFN-γ were determined using ELISA or cytometric bead array (BD Biosciences or Bio-Rad), as per the manufacturer's instructions. For empty LN predosing studies, C57BL/6 mice were dosed i.v. with free mCpG ODN alone, empty LN alone, or with empty LN 0.5 h prior to the i.v. administration of free mCpG ODN at ODN and lipid doses of 20 and 200 mg/kg, respectively; tissue samples were collected at 4 and 24 h. Spleens and blood were processed and analyzed as previously described.

Flow cytometry

Cell uptake (as judged by the intensity of the fluorescently labeled ODN on a per-cell basis) was assessed in specific immune cell populations (as determined by phenotype analysis; cell suspensions were stained with PE-conjugated anti-CD11b or allophycocyanin-conjugated anti-CD11c Abs, and analyzed using a four-color FACSort flow cytometer and CellQuest Pro software, both from BD Biosciences). For a determination of immune activation, cell suspensions were stained with FITC- or allophycocyanin-labeled phenotype Abs (against CD11b, CD11c, Mac3, CD8, and B220/CD45R) in combination with PE-conjugated Abs directed against the activation markers CD69 or CD86. Cell activation was assessed using an LSRII flow cytometer and FACS Diva software (BD Biosciences).

Endosomal trafficking and localization

Endosomal localization of free and encapsulated CpG ODN and mCpG ODN was assessed by incubating RAW264.7 cells with 10 μg/ml free or encapsulated CpG ODN or mCpG ODN for 4 h prior to the addition of 1 mg/ml subcellular compartmental marker, Texas Red-conjugated dextran 10,000 m.w., for an additional 2 h. BMDCs were grown on poly-D-lysine–precoated coverslips and incubated with 5 μg/ml free or encapsulated CpG ODN or mCpG ODN for 4 h. To determine the possibility of preferential trafficking of unmethylated CpG ODN specifically to TLR9-containing endosomes, thus allowing for interaction with TLR9 and immunostimulatory activity compared with mCpG ODN, C57BL/6 mice were injected i.v. with 20 mg/kg free or encapsulated, methylated or unmethylated fluorescently labeled CpG ODN or 150 mg/kg DiI–labeled empty LNs. To demonstrate the role of SFK signaling in the colocalization of CpG ODN, LN-CpG ODN, and LN-mCpG ODN, C57BL/6 mice were initially injected i.p. with 1 mg/kg specific SFK inhibitor PP2 twice per day for 7 d. Following the last treatment, mice were injected i.v. with 20 mg/kg free or encapsulated, methylated or unmethylated fluorescently labeled CpG ODN. After 4 h, all mice were euthanized, spleens were

disrupted, and dendritic cells (DCs) were isolated and processed for visualization, as outlined previously.

Immunofluorescence

Following incubation, RAW264.7 cells were washed and incubated in Optimem prior to live cell visualization. BMDCs were treated with 2% BSA in PBS, fixed in 2% paraformaldehyde, and permeabilized with 0.1% saponin and 2% BSA in PBS. Cells were stained with rat anti-mouse LAMP1, followed by Alexa 647-conjugated rabbit anti-rat Ab as a detection reagent. For ex vivo studies, spleens were dissociated by injection of 1 ml RPMI 1640 containing 5% FBS and 1 mg collagenase D and incubated for 30 min at 37˚C. Subsequently, DC-enriched cell populations were obtained by centrifugation of cell suspensions on Ficoll-Paque gradients. DCs were then purified by positive selection with anti-CD11c MACS beads, with the resulting population being >98% $CD11c^+$. Splenic DCs were resuspended in complete media and grown on poly-D-lysine–precoated coverslips for 3 h. Attached DCs were then treated with 2% BSA in PBS, followed by fixation with 2% paraformaldehyde. The cells were then permeabilized with 0.1% saponin and 2% BSA in PBS, followed by incubation with goat anti-mouse EEA1 or rat anti-mouse LAMP1. Secondary Alexa 647-conjugated rabbit anti-goat and goat anti-rat Abs were used, as detection reagents. To examine the colocalization of EEA1 and $LAMP1^+$ compartments with TLR3, TLR7, or TLR9, mouse anti-mouse or rabbit anti-mouse TLR3, TLR7, or TLR9 polyclonal Abs, followed by rabbit anti-mouse and or goat anti-rabbit, both coupled to Alexa 568 were used, respectively.

Confocal microscopy

For RAW264.7 and BMDCs, sections 0.1 μm in thickness were captured using a Bio-Rad Radiance 2000 laser scanning or Nikon C1 immunofluorescent confocal microscope. Data were analyzed using ImageJ v1.37 (National Institutes of Health, Bethesda, MD), to select images with a total thickness of 0.2–0.3 μm, and processed with Adobe Photoshop CS2 (Adobe Systems, San Jose, CA). For ex vivo studies, sections of 0.15 μm were captured with a Nikon-C1, TE2000-E immunofluorescent confocal microscope (Nikon Instruments, Melville, NY). Data were analyzed as described previously, and stacks with a total thickness of 0.6 μm were processed with Adobe Photoshop CS2. Isotype control Abs were used in all confocal microscopy experiments to confirm the specificity of Ab staining. Thirty to 50 images were collected for each treatment. The percentage of colocalization of combinations of free or encapsulated CpG ODN or mCpG ODN, TLR9, and LAMP1/EEA1, for all studies, was assessed in OpenLab (PerkinElmer, Woodbridge, Ontario, Canada).

Statistical analyses

All statistical analyses were performed using SPSS version 14.0 (SPSS, Chicago, IL). Initially, one-way ANOVA was used to statistically evaluate the differences among treatment groups. In the case of statistically significant results, unless otherwise stated, the differences among treatment groups were assessed through the use of Bonferroni adjusted *t* tests, a post hoc test that controls for family-wise error rate. A p value <0.05 was considered significant.

Results

Methylation status does not influence ODN uptake or intracellular trafficking by immune cells when in free or LN-encapsulated form

The uptake and trafficking characteristics of unmethylated and methylated CpG ODN were assessed to clarify their roles as determinants of immunostimulatory activity. Results from in vitro uptake studies of fluorescently labeled ODN in cultured macrophage cells and BMDCs demonstrated that, regardless of the duration of exposure or ODN concentration (Supplemental Fig. 1), free mCpG ODN and CpG ODN are taken up in a similar manner in both cell types (Fig. 1*Aa*, 1*Ab*, respectively; Supplemental Fig. 4*A*). Likewise, an in vivo analysis of uptake following s.c. administration of labeled ODN (Fig. 1*B*, Supplemental Fig. 4*A*) showed that free unmethylated and methylated CpG ODN are taken up similarly by APCs, as demonstrated in $CD11b^+$ cells (Fig. 1*Ba*, 1*Bc*), $CD11c^+$ cells (Fig. 1*Bb*, 1*Bd*), and, to a lesser extent, $B220^+$ cells (Supplemental Fig. 2) from spleen (Fig. 1*Ba*, 1*Bb*, Supplemental Fig. 2*A*) and lymph nodes (Fig. 1*Bc*, 1*Bd*, Supplemental Fig. 2*B*). As expected, similar uptake for LN-encapsulated unmethylated and methylated ODN was also observed in vitro and in vivo.

Intracellular trafficking was also evaluated for a potential role in determining the relative immunostimulatory activities of CpG and mCpG ODN. Endosomal trafficking was assessed in RAW264.7 cells and BMDCs (data not shown) using the fluid-phase subcellular compartmental marker Texas Red-conjugated dextran in conjunction with fluorescently labeled ODN. As shown in Fig. 2*A*, mCpG and CpG ODN efficiently localized to the endosomal compartment in free (Fig. 2*Aa*, 2*Ab*) or LN (Fig. 2*Ac*, 2*Ad*) form. Similarly, free and LN-mCpG and CpG ODN were delivered efficiently to the endosomal compartment of BMDCs, as shown by the colocalization with EEA1 (data not shown) and $LAMP1^+$ (Fig. 2*B*). As expected, uptake and trafficking were not dependent on CpG motifs, because non-CpG ODN exhibited identical in vitro and in vivo uptake and intracellular trafficking characteristics (data not shown).

Free CpG, LN-CpG, and LN-mCpG ODN colocalize with TLR9 in the late endosomal compartment, but free mCpG does not

The similar uptake and endosomal trafficking characteristics indicate that the differential immunostimulatory activity of free unmethylated and methylated CpG ODN cannot be attributed to either of these two processes. To evaluate the potential impact of other aspects of intracellular trafficking on immunostimulatory activity, an ex vivo examination of the relative ability of free CpG and mCpG ODN to colocalize with TLR9 in the endosomal compartment was undertaken. Specifically, the colocalization of CpG ODN with TLR9 in early and late endosomes was assessed in DCs isolated from the spleens of mice injected with fluorescently labeled free unmethylated or methylated CpG ODN.

Consistent with immunostimulatory activity, mice treated with free CpG ODN showed colocalization of CpG ODN with TLR9 in the $LAMP1^+$ compartment (Fig. 3*Ab*) but not for free mCpG ODN (Fig. 3*Aa*), whereas the administration of CpG ODN encapsulated in LNs resulted in effective colocalization with TLR9 in the late endosomal compartment, regardless of ODN methylation status (Fig. 3*Ac*, 3*Ad*). Quantitative analysis (Fig. 3*B*, Supplemental Fig. 4*B* for combined data) and statistical analyses confirmed that free CpG ODN (16.8% ± 4.0%), as well as LN-CpG (24.1% ± 6.8%) and LN-mCpG ODN (22.3% ± 6.6%), effectively colocalized with TLR9 in the late endosome, whereas free mCpG ODN (7.3% ± 3.2%) did not ($p < 0.001$ for all three compared with free mCpG ODN). Of note, LN-mCpG ODN and LN-CpG ODN demonstrated significantly greater colocalization with TLR9 in $LAMP1^+$ compartments than did free CpG ODN ($p < 0.05$ and $p < 0.001$, respectively), with no difference in colocalization between the two encapsulated forms. Interestingly, the uptake of LNs themselves, regardless of payload, seems to be a sufficient trigger for colocalization, because empty LNs administered i.v. colocalized with TLR9 in $LAMP1^+$ endosomes (Fig. 4*Ba*). The empty LNs labeled with the fluorescent marker DiI showed statistically significantly greater colocalization with TLR9 in the $LAMP1^+$ compartment (17.2% ± 5.7%) compared with free mCpG ODN ($p < 0.001$).

Significantly greater colocalization of CpG ODN with TLR9 occurred in late $LAMP1^+$ endosomes (Fig. 3*Ca*) compared with early $EEA1^+$ endosomes following the administration of free CpG, LN-CpG, and LN-mCpG ($p < 0.001$, $p < 0.05$, and $p < 0.001$, respectively). This is despite the fact that similar levels of free and LN-CpG ODN are found in early and late endosomes (Fig. 3*Cb*).

These data show that the ability of free CpG ODN to colocalize with TLR9 in late endosomes is dependent on methylation status and that delivery in LN form overcomes this discrimination and

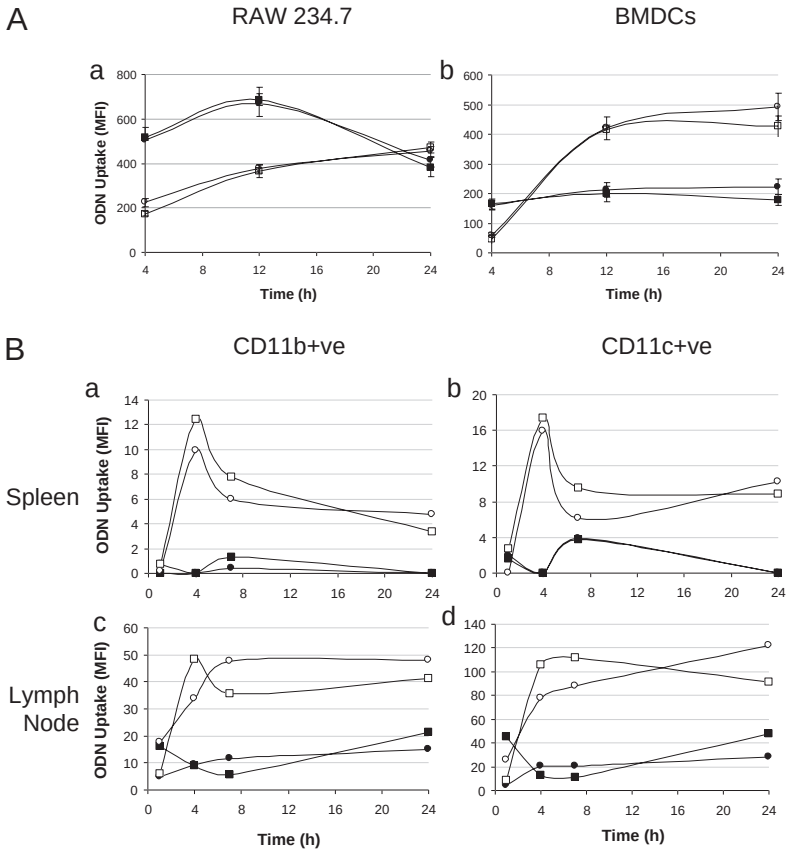

FIGURE 1. The uptake of free and LN-encapsulated CpG ODN is not influenced by the methylation status of the ODN. *A*, In vitro uptake of free and LN unmethylated and methylated CpG ODN by murine RAW264.7 macrophage cells and BMDCs. RAW264.7 cells (*Aa*) and BMDCs (*Ab*) were incubated with 10 and 5 μg/ml of fluorescently labeled (5-FAM) free mCpG ODN (●), free CpG ODN (■), LN-mCpG ODN (○), or LN-CpG ODN (□), respectively. Cells were analyzed for uptake of ODN (as judged by MFI) by flow cytometry. Levels of uptake at 4˚C and background fluorescence levels were subtracted from the data (MFIs of 54 for mCpG ODN, 64 for CpG ODN, 2.7 for LN-mCpG ODN, and 2.9 for LN-CpG ODN [*Aa*] and MFIs of 22 for mCpG ODN, 26 for CpG ODN, 4.2 for LN-CpG ODN, and 5.1 for LN-mCpG ODN [*Ab*]). Data are representative of three separate experiments. The combined data for in vitro ODN uptake in RAW234.7 and BMDCs are shown in Supplemental Fig. 4*A*. *B*, In vivo uptake of free and LN unmethylated and methylated CpG ODN by spleen- and lymph node-resident immune cells. Fluorescently labeled (5-FAM) free mCpG ODN (●), free CpG ODN (■), LN-mCpG ODN (○), and LN-CpG ODN (□) was administered s.c. to mice (four animals/group). Mice were euthanized at the indicated time points, and spleens (*Ba*, *Bb*) and lymph nodes (*Bc*, *Bd*) were harvested and processed to single cells. Samples were analyzed for uptake of the ODN (as judged by MFI) by specific cell types (as judged by expression of the phenotype markers CD11b [*Ba*, *Bc*] and CD11c [*Bb*, *Bd*]) by flow cytometry. Background fluorescence levels (MFIs of 18.1, 17.8, 11.8, and 13.2 for *Ba–d*, respectively) were subtracted from the data. Data are representative of at least three independent experiments. The combined data for in vivo ODN uptake in splenic and lymph node CD11b and CD11c cells are shown in Supplemental Fig. 4*A*.

allows for colocalization, regardless of the methylation status (or even the presence) of the payload.

Colocalization with TLR9 and immunostimulatory activity are mediated via SFK

It was reported that CpG motifs induce a sequence-specific, TLR9-independent SFK-signaling cascade at the plasma membrane that is ultimately required for CpG engagement and the activation of TLR9-MyD88 (21). Therefore, we investigated whether SFK signaling could mediate the colocalization of free CpG ODN (and potentially, LN-CpG and LN-mCpG ODN) with TLR9 in the LAMP1$^+$ compartment. To demonstrate the role of SFK signaling in colocalization, mice were pretreated with PP2, an SFK-specific inhibitor, prior to the administration of fluorescently labeled free or encapsulated CpG ODN and mCpG ODN.

As shown in Fig. 4*A*, pretreatment with PP2 effectively abolished the colocalization of free CpG ODN with TLR9 in the endosomal compartment compared with untreated controls (Fig. 4*Ab* versus 4*Aa*; 2.6% ± 3.2% compared with 16.1 ± 8.1%; $p < 0.001$). Similarly, PP2 was effective in preventing colocalization of TLR9 with LN-CpG ODN (Fig. 4*Ac*; 4.7% ± 5.4%) and LN-mCpG ODN (Fig. 4*Ad*; 2.7% ± 1.7%) in LAMP1$^+$ compartments, as well as with empty LNs (Fig. 4*Bb*; 17.3% ± 5.7%) compared with non–PP2-treated controls (Fig. 4*Ba*; 1.3% ± 1.7%). Quantitative data for the free and LN unmethylated and methylated CpG and for empty LNs are shown in Fig. 4*Ca* and 4*Ab*, respectively (Supplemental Fig. 4*B* for combined data). Concomitant with a significant reduction in the colocalization of free CpG ODN, LN-CpG ODN, and LN-mCpG ODN with TLR9 in the late endosomal compartment following treatment with PP2, a reduction in immune cell activation and cytokine secretion was observed (Fig. 5*A*, 5*B*, respectively; Supplemental Fig. 4*C* for combined data). The most notable effects of SFK suppression resulting from the administration of PP2 were on the upregulation of CD86 and CD69 on Mac3$^+$ and CD11c$^+$ cells. As shown in Fig. 5*A*, a significant reduction was observed in the expression of CD69 on Mac3$^+$ (Fig. 5*Ac*; $p < 0.05$ and $p < 0.005$ for free and encapsulated CpG ODN, respectively), CD8$^+$ (Fig. 5*Ad*; $p < 0.05$ for encapsulated CpG ODN), and CD11c$^+$ cells (Supplemental Fig. 3, $p < 0.005$) and the expression of CD86 on B220$^+$ (Fig. 5*Ab*; $p < 0.05$ and $p < 0.001$ for free and encapsulated CpG ODN, respectively) and CD11c$^+$ cells (Fig. 5*Aa*; $p < 0.05$ for free

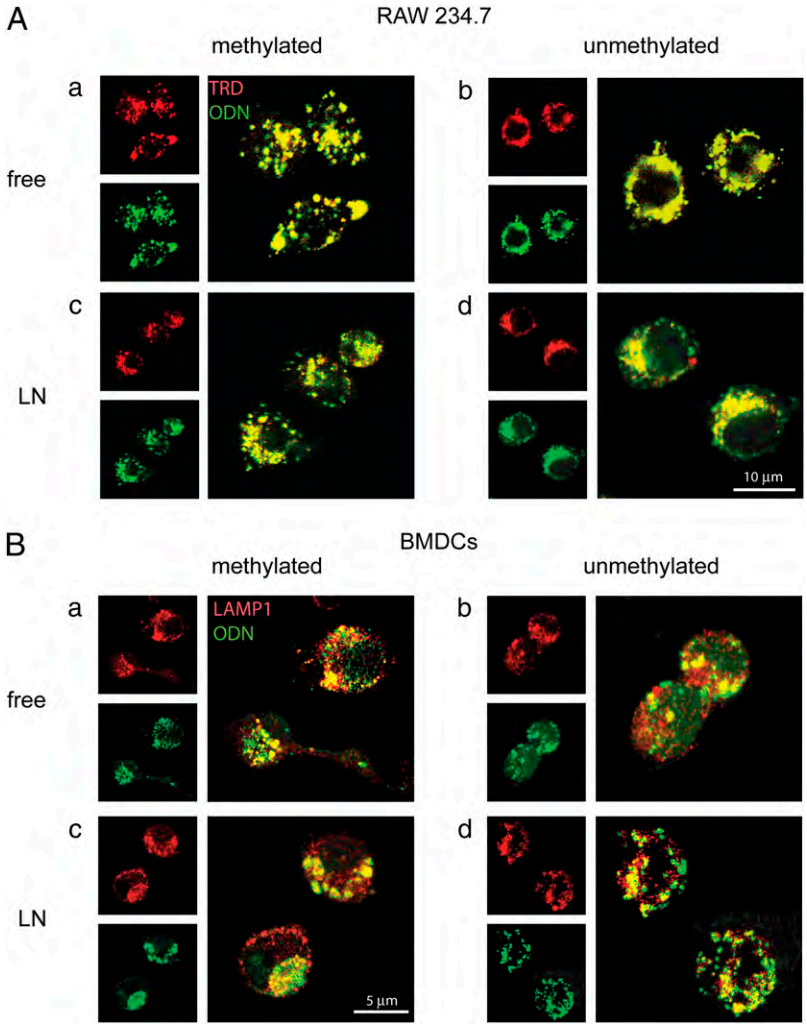

FIGURE 2. The trafficking of free and LN-encapsulated CpG ODN is not influenced by the methylation status of the ODN. *A*, Fluorescent confocal micrographs showing CpG ODN trafficking to the endosomal compartment in RAW264.7 cells. RAW264.7 cells were incubated with fluorescently labeled free mCpG ODN (*Aa*), free CpG ODN (*Ab*), LN-mCpG ODN (*Ac*), or LN-CpG ODN (*Ad*), followed by the addition of the fluid-phase endosomal marker Texas Red-conjugated dextran. Cells were analyzed by confocal microscopy for trafficking of CpG ODN to the endosomal compartment. Images represent Z-compressions of one or two sequential sections. *B*, Fluorescent confocal micrographs showing CpG ODN trafficking to endosomal compartment in BMDCs. BMDCs were incubated with fluorescently labeled free mCpG ODN (*Ba*), free CpG ODN (*Ba*), LN-mCpG ODN (*Bc*), or LN-CpG ODN (*Bd*). After fixation, late endosomes were stained with an anti-LAMP1 Ab prior to imaging by confocal microscopy for trafficking of CpG ODN to the LAMP1$^+$ endosomal compartment. Images were captured under ×60 oil immersion and represent Z-compres sions of one or two sequential sections.

and encapsulated CpG ODN). Similarly, a significant decrease in the secretion of cytokines was also observed (Fig. 5*b*), with an almost 10-fold reduction in IFN-γ, a 6-fold reduction in IL-6, and a 50% reduction in MCP-1 following the administration of PP2 (Fig. 5*Ba–c*, respectively).

Free CpG ODN and encapsulated CpG and mCpG ODN enable colocalization by inducing TLR9 mobilization to LAMP1$^+$ endosomes

Although the preceding data implicate SFK-mediated differential colocalization in the late endosomal compartment as a factor in determining the immunostimulatory activity of methylated and unmethylated, free and encapsulated CpG ODN, they do not resolve whether the differential colocalization is due to free CpG ODN, LN-CpG, and LN-mCpG ODN trafficking specifically to TLR9-containing endosomes or, conversely, TLR9 mobilization to the endosomal compartment. To investigate these possibilities, the trafficking behavior of TLR9 and ODN to the endosomal compartment was assessed. Results shown in Fig. 6*A* indicate that TLR9 mobilizes and localizes within LAMP1$^+$ compartments following treatment with CpG-ODN (Fig. 6*Ab*; 23.5% ± 6.0%), LN-mCpG ODN (Fig. 6*Ad*; 43.1% ± 10.5%), and LN-CpG ODN (Fig. 6*Af*; 39.6% ± 6.0%) but not free mCpG ODN (Fig. 6*Aa*; 12.3% ± 8.0%) ($p < 0.001$ for all treatments compared with mCpG ODN). This was confirmed with PP2 studies. Consistent with data from SFK-inhibition studies (Fig. 3*Ab–d*), treatment with PP2 resulted in a parallel decrease in TLR9 mobilization to late endosomes (Fig. 6*Ac*, *6Ae*, 6*Ag*, for free CpG ODN, LN-mCpG ODN, and LN-CpG ODN, respectively; $p < 0.001$ in all cases compared with untreated animals). Quantitative data for TLR9 mobilization to late endosomes are shown in Fig. 6*Ba*. Empty LNs also promoted the localization of TLR9 in LAMP1$^+$ compartments (30.4% ± 6.3%), which was inhibited by PP2 (5.3% ± 3.7%) (Fig. 6*Ah*, 6*Ai*), indicating that these empty particles affect TLR9 trafficking in a similar manner. Conversely, no significant differences were observed in the trafficking of methylated versus unmethylated CpG ODN, in free or encapsulated forms, to the late endosomal compartment (Fig. 6*Bb*), which was also unaffected by the inhibition of SFK signaling. Combined data for TLR9/ODN and LAMP1 colocalization studies are shown in Supplemental Fig. 4*D*. These data indicate that the administration of free CpG (but not mCpG) ODN, as well as LN, promotes an SFK-dependent mobilization of TLR9 to LAMP1$^+$ compartments that is responsible for colocalization rather than differential CpG trafficking.

It is notable that LN-CpG and LN-mCpG ODN induce significantly greater mobilization of TLR9 to the endosomal compartment compared with an equivalent dose of free CpG ODN (43.1% ± 6.0% versus 23.5% ± 6.0% [$p < 0.001$] and 39.6% ± 10.5% versus 23.5% ± 6.0% [$p < 0.001$], respectively). Although we previously attributed the enhanced immunostimulatory activity of encapsulated versus free CpG ODN to improved delivery and uptake by APCs, the enhanced mobilization of TLR9, leading to increased levels in the late endosomal compartment, may be another contributing factor.

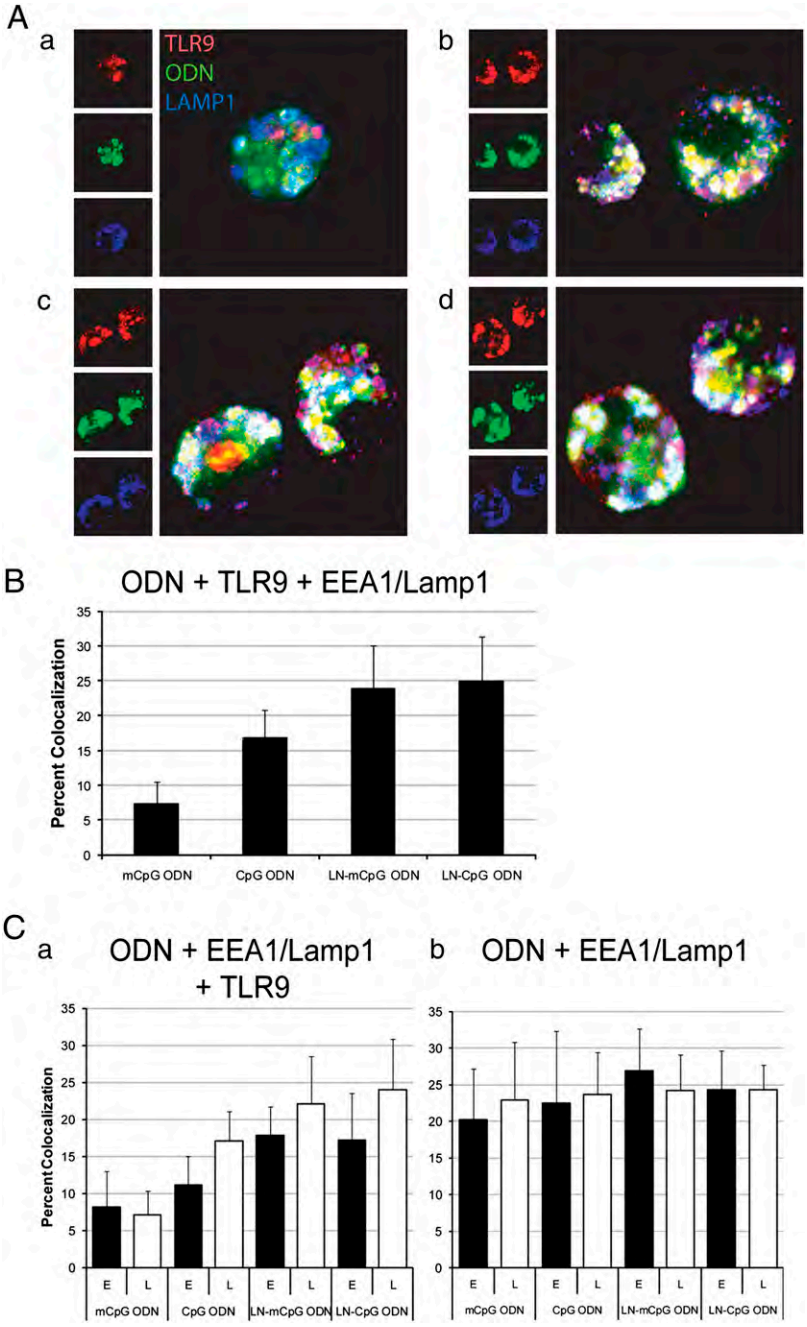

FIGURE 3. Free CpG, LN-CpG, and LN-mCpG ODN colocalize with TLR9 in LAMP1$^+$ compartments in vivo, but free mCpG ODN does not. *A*, Fluorescent confocal micrographs showing CpG ODN–TLR9 colocalization in LAMP1$^+$ endosomes of splenic DCs. Fluorescently labeled free mCpG ODN (*Aa*), free CpG ODN (*Ab*), LN-mCpG ODN (*Ac*), or LN-CpG ODN (*Ad*) was administered i.v. to mice (five animals/group). Animals were euthanized, spleens were harvested, and CD11c$^+$ cells were isolated and permeabilized. After fixation, cells were stained directly with anti-TLR9 and anti-LAMP1 (late endosomal marker protein) Abs and imaged by confocal microscopy for colocalization of CpG ODN with TLR9 in LAMP1$^+$ endosomes. Images were captured under ×60 oil immersion and represent Z-compressions of three or four sequential sections. Data are representative of at least three independent experiments. *B*, Colocalization of CpG ODN with TLR9 in LAMP1$^+$ endosomes of splenic DCs. Cells were visualized using confocal microscopy. Colocalization of fluorescently labeled ODN, TLR9, and LAMP1 (percentage of colocalization ± SD) was quantified using OpenLab. Data are representative of three separate experiments. The combined colocalization data in splenic DCs are shown in Supplemental Fig. 4*B*. *C*, Colocalization of free CpG, LN-CpG, and LN-mCpG ODN with TLR9 occurs predominantly in LAMP1$^+$ compartments in vivo. Fluorescently labeled free and LN-mCpG and CpG ODN was administered i.v. to mice (five animals/group). After 4 h, animals were euthanized, spleens were harvested, and CD11c$^+$ cells were isolated and permeabilized. After fixation, cells were stained directly with Abs directed against the early (E) EEA1 or the late (L) LAMP1 endosomal markers in the presence (*Ca*) or absence (*Cb*) of Abs against TLR9 and imaged by confocal microscopy; the percentage of colocalization ± SD was quantified using OpenLab. Data are representative of at least three independent experiments.

Predosing with empty LNs endows immunostimulatory activity on free mCpG ODN

Overall, these data indicated that the immunostimulatory activity of CpG DNA (free unmethylated, as well as LN-CpG and mCpG) is dependent on its ability to induce TLR9 mobilization to the late endosomal compartment rather than its receptor-binding affinity. In contrast, free mCpG ODN fails to induce mobilization and, thus, is immunologically inactive. Based on this model of CpG DNA/TLR9 activity, it can be predicted that if TLR9 were present in the endosomal compartment, free CpG ODN, regardless of methylation status, would be immunostimulatory. Therefore, to confirm our hypothesis, we tested this prediction by predosing mice with empty LNs to mobilize TLR9 to the endosomal compartment prior to treatment with free mCpG ODN.

As previously demonstrated, the administration of free mCpG ODN or empty LNs failed to induce immune stimulation, as assessed by immune cell activation at 4 or 24 h (Fig. 7*A*). However, as predicted, the administration of empty liposomes, followed 0.5 h later by free mCpG ODN, induced the expression of the activation markers CD69 (Fig. 7*Aa*, 7*Ac*, 7*Ae*, 7*Ag*) and CD86 (Fig. 7*Ab*, 7*Ad*, 7*Af*) in a number of immune cell populations, including CD11b$^+$ (Fig. 7*Aa*, 7*Ab*), CD11c$^+$ (Fig. 7*Ac*, 7*Ad*), CD45R/B220$^+$ (Fig. 7*Ae*, 7*Af*), and DX5$^+$ (Fig. 7*Ag*) cells by 24 h, compared with control animals, as well as those treated with mCpG ODN and empty liposomes alone ($p < 0.001$ for all groups and parameters measured). A similar and statistically significant upregulation of cell-activation marker expression on all immune cell populations examined was seen on a per-cell basis, as judged by mean fluorescence intensity (MFI) (Supplemental Fig. 5).

Consistent with these data, the analysis of plasma cytokine levels showed that pretreatment with empty LNs endowed immune activity on free mCpG ODN. Plasma levels of IL-6 ($p < 0.001$) and

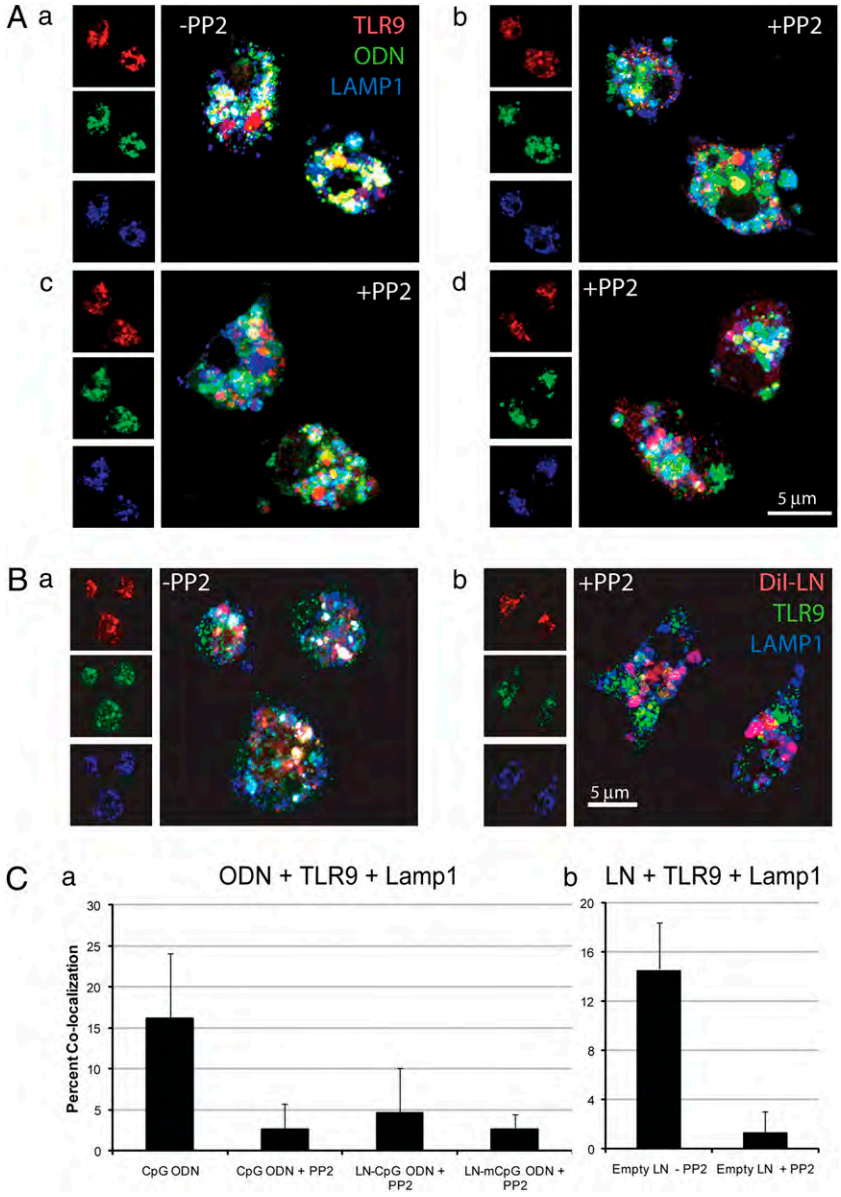

FIGURE 4. SFK inhibitor PP2 inhibits the localization of TLR9 to LAMP1$^+$ endosomes. *A*, Fluorescent confocal micrographs showing inhibition of CpG ODN and TLR9 colocalization in LAMP1$^+$ endosomes of splenic DCs by PP2. C57BL/6 mice (five animals/group) were treated i.p. with PP2. Following the final treatment, mice were injected i.v. with fluorescently labeled free CpG ODN (*Aa*, *Ab*), LN-CpG ODN (*Ac*) or LN-mCpG ODN (*Ad*) in control (*Aa*) or PP2-treated (*Ab–d*) mice. Animals were euthanized, spleens were harvested, and CD11c$^+$ cells were isolated and permeabilized. After fixation, cells were stained directly with anti-TLR9 and LAMP1 Abs and imaged by confocal microscopy for colocalization of CpG ODN with TLR9 in LAMP1$^+$ endosomes. Images were captured under ×60 oil immersion and represent Z-compressions of three or four sequential sections. Data are representative of two separate experiments. *B*, Fluorescent confocal micrographs showing colocalization of empty LNs with TLR9 in LAMP1$^+$ endosomes of splenic DCs. C57BL/6 mice (five animals/group) were initially treated i.p. with PP2. Following final treatment, DiI-labeled empty LNs were administered i.v. to control (*Ba*) and PP2-treated (*Bb*) mice. Animals were euthanized, spleens were harvested, and CD11c$^+$ cells were isolated and permeabilized. After fixation, cells were stained directly with anti-TLR9 and anti-LAMP1 Abs and imaged by confocal microscopy for colocalization of empty LNs with TLR9 in LAMP1$^+$ endosomes. Images captured under ×60 oil immersion. Data are representative of two separate experiments. *C*, Inhibition of CpG ODN or LN colocalization with TLR9 in LAMP1$^+$ endosomes of splenic DCs by PP2. Cells were visualized by confocal microscopy, and colocalization of fluorescently labeled ODN or LN with TLR9 and LAMP1 (percentage of colocalization ± SD) was quantified using OpenLab. Data are representative of two separate experiments. The combined colocalization data in splenic DCs are shown in Supplemental Fig. 4*B*.

IL-12p70 ($p < 0.001$) at 4 h and IFN-γ ($p < 0.001$) and MCP-1 ($p < 0.01$) at 24 h were significantly elevated compared with control animals (Fig. 7*Ba–d*, respectively), as well as those treated with mCpG ODN and empty liposomes alone, for which little or no effect was observed. Similar data were observed at 4 and/or 24 h following administration for the majority of other cytokines, chemokines, and growth factors examined, including IL-1, -3, -4, and -10; TNF-α; MIP-1α; RANTES; G-CSF; and GM-CSF, whereas treatment with free mCpG ODN or empty LNs generally did not result in significant changes in plasma cytokine levels compared with those observed for the saline-treated control.

Additional studies were used to further test this hypothesis with various other CpG ODNs, including INX-5001, a hexameric CpG ODN, and CpG 2006, a human optimized 24mer containing three CpG motifs. As clearly shown (Supplemental Fig. 6), although empty LNs or free mCpG ODN alone was not immunostimulatory, the administration of LNs followed by free mCpG ODN resulted in the activation of a variety of immune cell populations, including macrophages, DCs, B lymphocytes, and NK cells. The similar results from these studies demonstrating that prearming endosomes with TLR9 endows otherwise inactive, free mCpG ODN with immune activity further validates this hypothesis and confirms it as a general model for determining unmethylated versus methylated CpG DNA/TLR9 immune activity.

Discussion

Eukaryotic organisms have evolved systems to rapidly elaborate protective immune responses to combat pathogenic invasion based on PRRs that recognize highly conserved molecular patterns associated with pathogens. Although most PRRs bind ligands that are structurally complex and unique, TLR9 recognizes CpG motifs within pathogenic DNA and synthetic ODNs. Distinguishing pathogenic sequences from eukaryotic DNA has been proposed to be a multifactorial process based, in part, on methylation status; it is generally accepted that TLR9 specifically recognizes unmethylated CpG motifs, and methylated DNA is nonimmunostimulatory because of its inability to interact with TLR9 (2, 10, 11, 13, 22). Recently, however, several separate lines of research indicated that mCpGs are able to induce immune responses via TLR9 (9, 14, 15), including work from this laboratory demonstrating that LN delivery endows mCpG ODN with immunostimulatory potential through a TLR9-dependent mechanism (17).

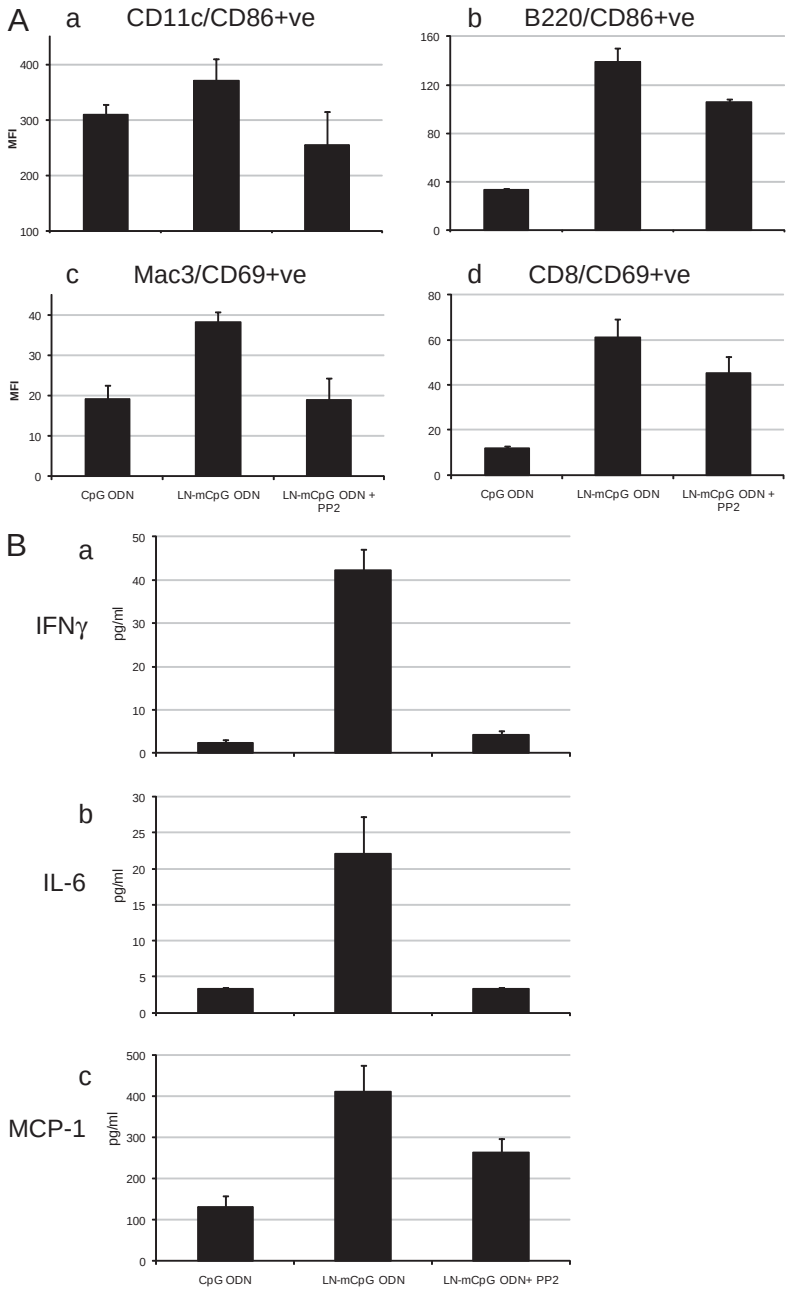

FIGURE 5. CpG-mediated immune stimulation is an SFK-dependent process. *A*, Inhibition of CpG-mediated cell activation marker expression on APCs by PP2. C57BL/6 mice (four animals/group) were treated i.p. with PP2. Following the final treatment, free or LN-CpG ODN was administered i.v. to mice. After 12 h, animals were euthanized, and spleens were harvested. Splenocytes were analyzed for the expression of CD69 and CD86 cell surface-activation markers in conjunction with phenotype markers by flow cytometry. Background MFI levels in the absence of CpG ODN of 80.1, 34.0, 8.2, and 6.7 were subtracted from the data presented in *Aa–d*, respectively. Data are representative of three separate experiments. The combined activation marker expression data on splenic immune cells are shown in Supplemental Fig. 4*C*. *B*, Inhibition of CpG-mediated plasma cytokine levels by PP2. C57BL/6 mice (four animals/group) were treated i.p. with PP2. Following the final treatment, free or LN-CpG ODN was administered i.v. to mice. After 12 h, animals were euthanized, blood was collected by cardiac puncture and processed to collect plasma, and levels of IFN-γ (*Ba*), IL-6 (*Bb*), and MCP-1 (*Bc*) were determined by cytometric bead array. Data are representative of three separate experiments. The combined plasma cytokine data are shown in Supplemental Fig. 4*C*.

These results showed that mCpG ODN can act through TLR9 to stimulate an immune response and indicated that the immunostimulatory activity of unmethylated versus methylated CpG ODN is regulated by a mechanism that does not involve differential TLR9 affinity. The data presented in this article show that the dependence of immunopotency on methylation status arises from the ability of free unmethylated (and the inability of free methylated) CpG ODN to induce TLR9 mobilization and colocalization in the late endosomal compartment via an SFK-signaling cascade. In contrast, nanoparticulate delivery allows for effective CpG ODN–TLR9 colocalization in late endosomes, regardless of methylation status, also via an SFK-signaling pathway, resulting in immunostimulatory activity. This was confirmed by studies in which the induction of TLR9 mobilization to the late endosomal compartment was sufficient to endow a range of free mCpG ODNs with immunostimulatory capacity.

Although the localization of TLR9 in the endoplasmic reticulum (ER) of resting APCs and its rapid trafficking to the endosomal/lysosomal compartments upon cellular activation have been well described (21), the mechanisms that control TLR9 trafficking are poorly understood. The data presented in this article demonstrating differential trafficking of TLR9 in response to free unmethylated and methylated CpG ODN points to a cellular mechanism that can distinguish CpG methylation status and trigger TLR9 mobilization, thus allowing for the colocalization of CpG ODN and TLR9 in the endosomal compartment, with subsequent binding and immunogenic signaling. Sanjuan et al. (21) reported on a CpG-dependent, TLR9-independent SFK-signaling pathway initiated by a plasma membrane-bound, sequence-specific receptor at the plasma membrane upstream of TLR9 that induces cytoskeletal reorganization and is ultimately required for TLR9 engagement and immunostimulatory activity. Although a definitive mechanistic answer awaits further studies, we propose that the

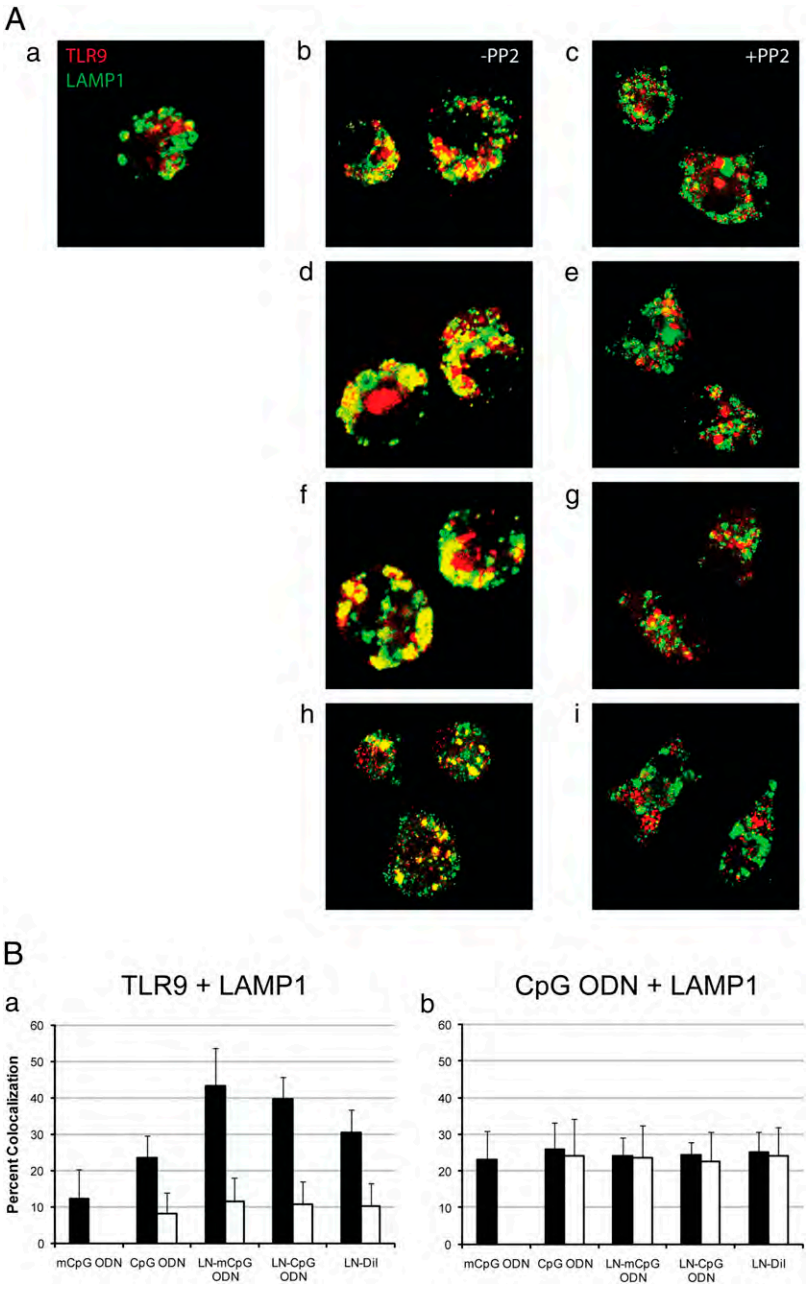

FIGURE 6. Colocalization is mediated by TLR9 mobilization and trafficking to the LAMP1$^+$ compartment. *A*, Fluorescent confocal micrographs showing TLR9 mobilization to LAMP1$^+$ endosomes of splenic DCs, which was inhibited by PP2. C57BL/6 mice (five animals/group) were treated i.p. with PP2 (*Ac*, *Ae*, *Ag*, *Ai*). Following the final treatment, free mCpG ODN (*Aa*), free CpG ODN (*Ab*, *Ac*), LN-mCpG OD 281–2150 N (*Ad*, *Ae*), LN-CpG ODN (*Af*, *Ag*), or DiI LN (*Ah*, *Ai*) was administered i.v. to mice. Animals were euthanized, spleens were harvested, and CD11c$^+$ cells were isolated and permeabilized. After fixation, cells were stained directly with anti-TLR9 and LAMP1 and imaged by confocal microscopy for TLR9 mobilization to LAMP1$^+$ endosomes. To enhance the ability to detect differences in colocalization, the color of the images was modified from magenta and cyan to red and green. Images were captured under ×60 oil immersion and represent Z-compressions of three or four sequential sections. Data are representative of two separate experiments. *B*, Mobilization of TLR9 and CpG ODN to LAMP1$^+$ endosomes of splenic DCs in control and PP2-treated mice. Cells were visualized by confocal microscopy and colocalization of immunostained TLR9 or fluorescently labeled ODN with LAMP1 (percentage of colocalization ± SD) was quantified using OpenLab. Black bars represent TLR9 or ODN and LAMP1$^+$ colocalization data from control animals, whereas white bars represent data from PP2-treated animals. Data are representative of two separate experiments. The combined colocalization data in splenic DCs are shown in Supplemental Fig. 4*D*.

SFK-mediated, methylation-dependent mobilization and migration of TLR9 described in this article and the pathway proposed by Sanjuan et al. (20) may represent a common pathway initiated by an unidentified surface receptor capable of distinguishing methylated versus nonmethylated and CpG versus non-CpG ODN.

It is noteworthy that LN uptake, regardless of payload, also acts via an SFK-signaling cascade to trigger TLR9 mobilization to the endosomal compartment, thus allowing methylated and unmethylated CpG ODN to colocalize with and engage TLR9. Although not capable of initiating an immune response (20, 23), LNs carrying no payload efficiently colocalize with TLR9 in LAMP1$^+$ compartments in an SFK-dependent manner. Although receptor-mediated and macropinocytotic/phagocytic uptake of free and LN-CpG ODN, respectively, represent distinct and divergent events, it seems likely that both processes converge through a common SFK-signaling cascade that results in TLR9 mobilization from the ER to the late endosome.

The results presented in this article suggest a new model whereby the relative immunopotency of unmethylated and methylated CpG and, by extension, self- and pathogenic DNA, is determined. In this model, free self-DNA liberated as a result of certain pathological conditions would fail to mobilize TLR9 and induce immune responsiveness, whereas advanced infections resulting in free pathogenic DNA would induce DNA–TLR9 colocalization and allow for immunostimulatory activity. Importantly, in the early stages of pathogenic infection in which the primary exposure to pathogenic DNA is likely to be through ingested bacterial and viral particles, phagocytic uptake would result in TLR9 mobilization and endosomal colocalization with pathogenic DNA, allowing for immunostimulatory responses. However, because a common route of exposure to self-DNA is through phagocytosis of apoptotic cells, additional mechanisms that specifically dampen immune responses to self-DNA acquired by phagocytosis are likely to be involved and could include receptors for lipid components unique to apoptotic cells, such as phosphatidylserine.

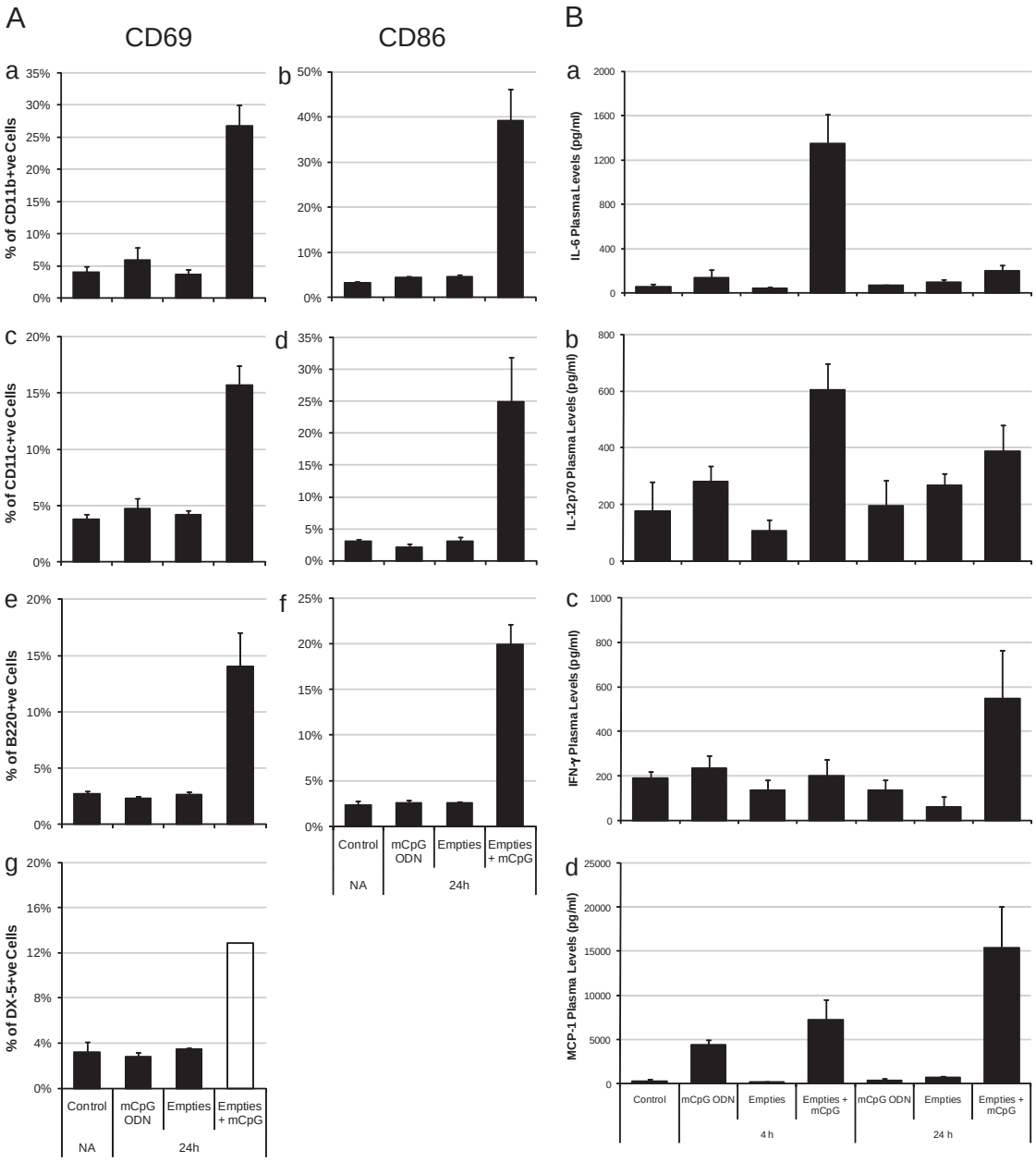

FIGURE 7. Predosing with empty LNs endowed free mCpG ODN with immunostimulatory activity. Immune activation in animals predosed with empty LNs prior to administration of free mCpG ODN. C57BL/6 mice (three animals/group) were treated i.v. with empty LNs followed 30 min later with free mCpG ODN. After 4 and 24 h, animals were euthanized, and blood and spleens were harvested. *A*, Cell activation-marker expression on immune cells 24 h after treatment with empty LNs prior to administration of free mCpG ODN. Splenocytes were analyzed for the expression of CD69 (*Aa*, *Ac*, *Ae*, *Ag*) and CD86 (*Ab*, *Ad*, *Af*, *Ah*) cell surface-activation markers in conjunction with CD11b (*Aa*, *Ab*), CD11c (*Ac*, *Ad*), CD45R/B220 (*Ae*, *Af*), and DX5 (*Ag*, *Ah*) phenotype markers by flow cytometry. *B*, Plasma cytokine/chemokine levels in animals 4 and/or 24 h after treatment with empty LNs prior to administration of free mCpG ODN. Blood was collected and processed to plasma for cytokine/chemokine/growth factor levels by multiplex bead array. Plasma levels are shown for the cytokines IL-6 (*Ba*) and IL12p70 (*Bb*) 4 h after administration and the cytokine IFN-γ (*Bc*) and chemokine MCP-1 (*Bd*) 24 h after administration.

Recently, it was proposed that the immunostimulatory activity of natural phosphodiester DNA via TLR9 is not dependent on the presence of CpG motifs, but rather is mediated by the deoxyribose backbone (24). Together with the findings reported in this article, these data seem to indicate that although DNA methylation impacts upstream events controlling TLR9 mobilization, it is not the methylation of CpG motifs, specifically, that is relevant.

In summary, we showed that TLR9-mediated recognition of bacterial DNA is more regulated than previously thought, with TLR9 being sequestered until activated by a stimulation provided by free unmethylated CpG DNA or particulate uptake. The results presented indicate that the SFK-dependent migration of TLR9 from the ER to the late endosomal/lysosomal compartment is a pivotal step for determining the immunostimulatory activity of free methylated and unmethylated CpG ODN, suggesting that the ability to distinguish self from non-self DNA does not reside within TLR9 itself, but rather occurs through strict regulation of its subcellular distribution. Similarly, particulate delivery, regardless of payload, primes APCs for immunostimulatory activity by promoting the SFK-dependent mobilization and trafficking of TLR9 from the ER to late endosomal compartments. Overall, our findings are consistent with work showing the importance of intracellular localization in regulating TLR9 activity and specificity (9), unify a number of concepts regarding TLR9-mediated immunostimulatory activity,

and provide insight into the mechanisms and processes that regulate TLR9 localization and signaling.

Finally, these results provide insight into the design of optimized, immune-based CpG clinical therapies, providing a mechanistic rationale for the administration of LN-mCpG ODN. Furthermore, results from this work may have direct implications in the development of other nucleic acid drugs, such as plasmid DNA for gene therapy and antisense, ribozyme, and siRNA oligonucleotides for targeted gene downregulation, which have significant requirements for systemic-delivery technologies. Understanding the mechanisms that regulate the immunostimulatory activity of particulate nucleic acids will provide guidance for the rational design, evaluation, and development of these therapeutics.

Disclosures

S.D.deJ. is an employee of Tekmira Pharmaceuticals Corporation, which is focused on the development of lipid-nanoparticulate nucleic acid therapeutics. P.R.C. is a founder of Tekmira, and P.R.C and Y.K.T. have financial interests in Tekmira.

References

1. Yamamoto, S., T. Yamamoto, S. Shimada, E. Kuramoto, O. Yano, T. Kataoka, and T. Tokunaga. 1992. DNA from bacteria, but not from vertebrates, induces interferons, activates natural killer cells and inhibits tumor growth. *Microbiol. Immunol.* 36: 983–997.
2. Krieg, A. M., A. K. Yi, S. Matson, T. J. Waldschmidt, G. A. Bishop, R. Teasdale, G. A. Koretzky, and D. M. Klinman. 1995. CpG motifs in bacterial DNA trigger direct B-cell activation. *Nature* 374: 546–549.
3. Klinman, D. M., A. K. Yi, S. L. Beaucage, J. Conover, and A. M. Krieg. 1996. CpG motifs present in bacteria DNA rapidly induce lymphocytes to secrete interleukin 6, interleukin 12, and interferon gamma. *Proc. Natl. Acad. Sci. USA* 93: 2879–2883.
4. Yi, A. K., J. H. Chace, J. S. Cowdery, and A. M. Krieg. 1996. IFN-gamma promotes IL-6 and IgM secretion in response to CpG motifs in bacterial DNA and oligodeoxynucleotides. *J. Immunol.* 156: 558–564.
5. Yi, A. K., D. M. Klinman, T. L. Martin, S. Matson, and A. M. Krieg. 1996. Rapid immune activation by CpG motifs in bacterial DNA. Systemic induction of IL-6 transcription through an antioxidant-sensitive pathway. *J. Immunol.* 157: 5394–5402.
6. Van Uden, J. H., C. H. Tran, D. A. Carson, and E. Raz. 2001. Type I interferon is required to mount an adaptive response to immunostimulatory DNA. *Eur. J. Immunol.* 31: 3281–3290.
7. Kaisho, T., and S. Akira. 2006. Toll-like receptor function and signaling. *J. Allergy Clin. Immunol.* 117: 979–987, quiz 988.
8. Ahmad-Nejad, P., H. Häcker, M. Rutz, S. Bauer, R. M. Vabulas, and H. Wagner. 2002. Bacterial CpG-DNA and lipopolysaccharides activate Toll-like receptors at distinct cellular compartments. *Eur. J. Immunol.* 32: 1958–1968.
9. Barton, G. M., J. C. Kagan, and R. Medzhitov. 2006. Intracellular localization of Toll-like receptor 9 prevents recognition of self DNA but facilitates access to viral DNA. *Nat. Immunol.* 7: 49–56.
10. Rutz, M., J. Metzger, T. Gellert, P. Luppa, G. B. Lipford, H. Wagner, and S. Bauer. 2004. Toll-like receptor 9 binds single-stranded CpG-DNA in a sequence- and pH-dependent manner. *Eur. J. Immunol.* 34: 2541–2550.
11. Takeshita, F., C. A. Leifer, I. Gursel, K. J. Ishii, S. Takeshita, M. Gursel, and D. M. Klinman. 2001. Cutting edge: Role of Toll-like receptor 9 in CpG DNA-induced activation of human cells. *J. Immunol.* 167: 3555–3558.
12. Bird, A. P., M. H. Taggart, R. D. Nicholls, and D. R. Higgs. 1987. Non-methylated CpG-rich islands at the human alpha-globin locus: implications for evolution of the alpha-globin pseudogene. *EMBO J.* 6: 999–1004.
13. Cornélie, S., J. Hoebeke, A. M. Schacht, B. Bertin, J. Vicogne, M. Capron, and G. Riveau. 2004. Direct evidence that toll-like receptor 9 (TLR9) functionally binds plasmid DNA by specific cytosine-phosphate-guanine motif recognition. *J. Biol. Chem.* 279: 15124–15129.
14. Yasuda, K., Y. Ogawa, I. Yamane, M. Nishikawa, and Y. Takakura. 2005. Macrophage activation by a DNA/cationic liposome complex requires endosomal acidification and TLR9-dependent and -independent pathways. *J. Leukoc. Biol.* 77: 71–79.
15. Yasuda, K., M. Rutz, B. Schlatter, J. Metzger, P. B. Luppa, F. Schmitz, T. Haas, A. Heit, S. Bauer, and H. Wagner. 2006. CpG motif-independent activation of TLR9 upon endosomal translocation of "natural" phosphodiester DNA. *Eur. J. Immunol.* 36: 431–436.
16. Yasuda, K., P. Yu, C. J. Kirschning, B. Schlatter, F. Schmitz, A. Heit, S. Bauer, H. Hochrein, and H. Wagner. 2005. Endosomal translocation of vertebrate DNA activates dendritic cells via TLR9-dependent and -independent pathways. *J. Immunol.* 174: 6129–6136.
17. Chikh, G., S. D. de Jong, L. Sekirov, S. G. Raney, M. Kazem, K. D. Wilson, P. R. Culllis, J. P. Dutz, and Y. K. Tam. 2009. Synthetic methylated CpG ODNs are potent in vivo adjuvants when delivered in liposomal nanoparticles. *Int. Immunol.* 21: 757–767.
18. Semple, S. C., S. K. Klimuk, T. O. Harasym, N. Dos Santos, S. M. Ansell, K. F. Wong, N. Maurer, H. Stark, P. R. Cullis, M. J. Hope, and P. Scherrer. 2001. Efficient encapsulation of antisense oligonucleotides in lipid vesicles using ionizable aminolipids: formation of novel small multilamellar vesicle structures. *Biochim. Biophys. Acta* 1510: 152–166.
19. Bligh, E. G., and W. J. Dyer. 1959. A rapid method of total lipid extraction and purification. *Can. J. Biochem. Physiol.* 37: 911–917.
20. de Jong, S., G. Chikh, L. Sekirov, S. Raney, S. Semple, S. Klimuk, N. Yuan, M. Hope, P. Cullis, and Y. Tam. 2007. Encapsulation in liposomal nanoparticles enhances the immunostimulatory, adjuvant and anti-tumor activity of subcutaneously administered CpG ODN. *Cancer Immunol. Immunother.* 56: 1251–1264.
21. Sanjuan, M. A., N. Rao, K. T. Lai, Y. Gu, S. Sun, A. Fuchs, W. P. Fung-Leung, M. Colonna, and L. Karlsson. 2006. CpG-induced tyrosine phosphorylation occurs via a TLR9-independent mechanism and is required for cytokine secretion. *J. Cell Biol.* 172: 1057–1068.
22. Latz, E., A. Schoenemeyer, A. Visintin, K. A. Fitzgerald, B. G. Monks, C. F. Knetter, E. Lien, N. J. Nilsen, T. Espevik, and D. T. Golenbock. 2004. TLR9 signals after translocating from the ER to CpG DNA in the lysosome. *Nat. Immunol.* 5: 190–198.
23. Li, W. M., M. B. Bally, and M. P. Schutze-Redelmeier. 2001. Enhanced immune response to T-independent antigen by using CpG oligodeoxynucleotides encapsulated in liposomes. *Vaccine* 20: 148–157.
24. Haas, T., J. Metzger, F. Schmitz, A. Heit, T. Müller, E. Latz, and H. Wagner. 2008. The DNA sugar backbone 2′ deoxyribose determines toll-like receptor 9 activation. *Immunity* 28: 315–323.